

CONF-830311--75

Los Alamos National Laboratory is operated by the University of California for the United States Department of Energy under contract W-7405-ENG-36

LA-UR--83-720

DE83 009963


TITLE: PULSED BEAM CHOPPER FOR THE PSR AT LAMPF

AUTHOR(S) J. S. Lunsford and R. A. Hardekopf

SUBMITTED TO 1983 Particle Accelerator Conference,
March 21-23, Santa Fe, NM

DISCLAIMER

This report was prepared as an account of work sponsored by an agency of the United States Government. Neither the United States Government nor any agency thereof, nor any of their employees, makes any warranty, express or implied, or assumes any legal liability or responsibility for the accuracy, completeness, or usefulness of any information, apparatus, product, or process disclosed, or represents that its use would not infringe privately owned rights. Reference herein to any specific commercial product, process, or service by trade name, trademark, manufacturer, or otherwise does not necessarily constitute or imply its endorsement, recommendation, or favoring by the United States Government or any agency thereof. The views and opinions of authors expressed herein do not necessarily state or reflect those of the United States Government or any agency thereof.

By acceptance of this article the publisher recognizes that the U.S. Government retains a nonexclusive, royalty-free license to publish or reproduce the published form of this contribution  to allow others to do so, for U.S. Government purposes.

The Los Alamos National Laboratory requests that the publisher identify this article as work performed under the auspices of the U.S. Department of Energy.

Los Alamos Los Alamos National Laboratory
Los Alamos, New Mexico 87545

ESH

PULSED BEAM CHOPPER FOR THE PSR AT LAMPF*

J. S. Lunsford and R. A. Hardekopf, AT-3, MS H806
Los Alamos National Laboratory, Los Alamos, NM 87545

Summary

A traveling-wave beam chopper has been designed to provide properly structured negative-ion beam to the Proton Storage Ring (PSR) and other LAMPF users. The chopper must provide a 20-mrad kick with pulse rise time <5 ns for the 750-keV H⁻ ions in the injector transport line. Variable pulse lengths from 15 ns to 750 μs at repetition rates up to 16.7 MHz must be generated in synchronization with the PSR circulation frequency. Parameter studies led to an optimized design combining good deflection efficiency and bandwidth with minimum deleterious effects from plate-to-plate coupling. Both positive and negative 600-V pulses, with lengths up to 1 ms and maximum 10% duty factor, can be generated to drive the deflectors.

Introduction

The Weapons Neutron Research Facility (WNR) presently receives a fraction of the LAMPF H⁺ beam, time-structured for one of two neutron-scattering modes. Beam chopping is accomplished in LAMPF's injector transport line by a traveling-wave deflector consisting of two helical structures with different pulsers for each operational mode.^{1,2} In 1985, when the PSR becomes operational, the WNR target will be able to receive beam either directly from LAMPF or with higher intensity and better time structure from the PSR. To provide the greater flexibility and higher duty factor required, we are developing a new chopping system consisting of high-efficiency deflection structures and pulse amplifiers with <5 ns rise time.

The traveling-wave deflection principle was discussed in Refs. 1 and 2. A rather long (~1-m) plate is needed to provide the 20-mrad deflection required by beam emittance and transport-line optics. The 750-keV ions travel at 1.2 cm/ns; thus, to get few-nanosecond rise times for the chopped beam, the deflecting pulse longitudinal velocity must be matched to the beam velocity. A helix structure, made by wrapping ground planes with turns of metal tape, has been used successfully for the WNR application but has some limitations that we hope to overcome:

- Turn-to-turn coupling produces precursors to the main pulse.
- Ceramic stand-offs for helix turns increase the coupling effect by introducing discontinuities in the transmission line.
- The deflection efficiency is poor because of a 35% aspect ratio (tape width divided by pitch) necessary to reduce coupling to an acceptable value.
- The copper tape sags with time, causing pulse distortion.

We compared measurements on the existing helix structure with calculational models, made parameter studies of deflection efficiency and bandwidth, and devised a more rugged mechanical structure with better pulse-propagation characteristics.

Deflector Efficiency Considerations

A previous theoretical study³ analyzed the frequency dependence of the helical structure and other design criteria, including beam optics. We

begin with this analysis because it elucidates the important factors in traveling-wave deflector design. The solution to the wave equation in rectangular coordinates for the helix geometry may be written as

$$E_y = \cos(k_z Z - \omega t) \left(\frac{V}{h}\right) \left(\frac{d}{\lambda}\right) \frac{\sin(k_z d/2) \cosh(k_y Y)}{k_z d/2 \cosh(k_y h/2)} \quad (1)$$

where two boundary conditions have been applied: $E_y = V/h$ adjacent to the tape and $E_y = 0$ in the space between windings. Also,

d = width of tape,

λ = spacing of tape (pitch),

h = spacing between helix structures,

k = wave number for frequency ω ,

V = potential applied to tape,

Z = distance along beam axis, and

Y = distance transverse to Z in deflection plane.

The efficiency on-axis ($Y=0$) at the position of the pulse is merely E_y divided by the dc field V/h , or

$$\text{Efficiency} = \left(\frac{d}{\lambda}\right) \frac{\sin(k_z d/2)}{k_z d/2} \frac{1}{\cosh(k_y h/2)} \quad (2)$$

The first term is the aspect ratio, or the fraction of deflection structure at potential V . The second term is the transit-time factor, which is very close to 1.0 for our geometry up to very high frequencies (>400 MHz). The third term is the beam-aperture factor, the major contributor to decreased efficiency for high-frequency pulses.

Laboratory Measurements

To evaluate the frequency response of the existing deflectors, designated Helix II,^{1,2} we constructed a grounded midplane and field probe. The probe was a rectangular strip of copper attached through a hole in the plane to a high-impedance FET pickup. A network analyzer was used to measure the frequency response, detailed in Ref. 4. For actual operating conditions of Helix II, h is ~2.8 cm; for a 200-MHz frequency, we measured ~0.6 rf efficiency compared with a 0.44 calculated value from the aperture factor.

The aspect-ratio term in Eq. (2), d/λ , is not frequency dependent but for Helix II contributes a factor of 0.35 to the calculated efficiency. We measured the field with the same probe but used the low frequency of 4 MHz where rf attenuation is negligible. The measurement was made by applying the 4-MHz signal first to the helix and then to the ground plane. The results show a 3-dB attenuation (0.7 ratio) for the helix compared to a continuous deflector.

Combining the results of the two measurements, we find the total efficiency of Helix II to be 42% compared to a calculated value from Eq. (2) of 15%.

Electrostatic Calculation

It is not surprising that measured and calculated values for the helix efficiency show such a large discrepancy when one considers the boundary conditions imposed to solve the wave equation in closed form. To improve the model, we used the code POISSON to solve the electrostatic problem by numerical integration. Figure 1 shows equipotential lines calculated

*Work supported by the US Department of Energy.

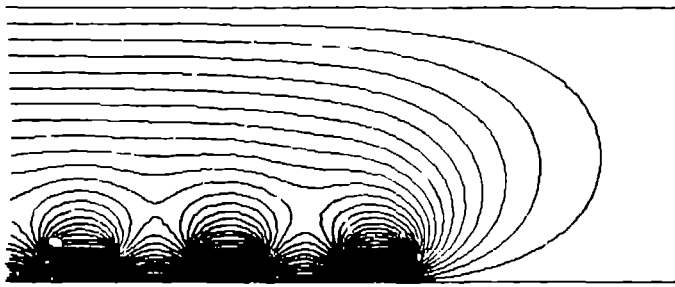


Fig. 1. POISSON calculation of equipotentials for three segments of Helix II. The Y-axis is vertical and the Z-axis is horizontal.

for a step-function voltage applied to a segment of Helix II. The steady-state electric field perpendicular to the tape (at the left of Fig. 1) is plotted in Fig. 2. This calculation shows that E_y on-axis ($Y = 1.6$ cm) is a factor of 0.7 of that for a continuous conductor, instead of the factor of 0.35 calculated at zero frequency from Eq. (2). Furthermore, this is exactly the 3-dB factor measured with the field probe. Additional calculations with variations of the width d of the segments, their spacing l , and their distance from the ground plane are represented by the curves in Fig. 3. The most important

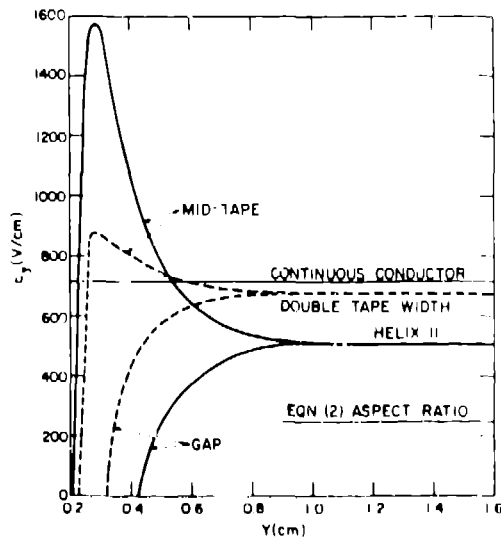


Fig. 2. Steady-state electric field calculated for Helix II with 1000-V applied voltage. POISSON results (curves) are compared to the analytical expression and to a continuous conductor.

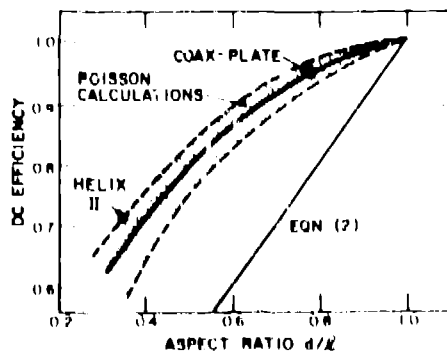


Fig. 3. The dc efficiency calculations, POISSON compared to the analytic expression. The shaded area is for different pitch parameters l .

parameter is still the aspect ratio, d/l , but the efficiency curves approach the linear approximation of Eq. (2) only in the continuous-plate limit.

Frequency-Dependent Calculation

If the POISSON result closely reproduces the measured value for the time-independent electric field, can a better calculation also be made for the frequency-dependent terms? Our approach was to investigate the wave front of Fig. 1 as we varied the structure's geometry. Because Eq. (2) indicates the most important frequency-dependent parameter to be the spacing h , we show (Fig. 4) the electric field at the deflection center line as a function of Z for four values of h . The slow-wave bandwidth is calculated from these figures by taking the difference in Z between the 10 and 90% E_y points, converted to rise time using the beam velocity. The equivalent frequency multiplied by 0.35 gives the deflection bandwidth to the -3-dB point. For the Helix II geometry, we show the results (Fig. 5) along with bandwidth calculated from the aperture factor of Eq. (2) and -3-dB points from the laboratory measurements. We find good agreement with the measurements and confirm that the frequency-dependent efficiency is better than the analytical solution predicts. We also confirm the primary importance of deflector spacing to the helix frequency response because variation of other parameters had only a minor effect on the calculated bandwidth.

Coax-plate Design

Along with the parameter studies, we made laboratory investigations to find a deflecting structure

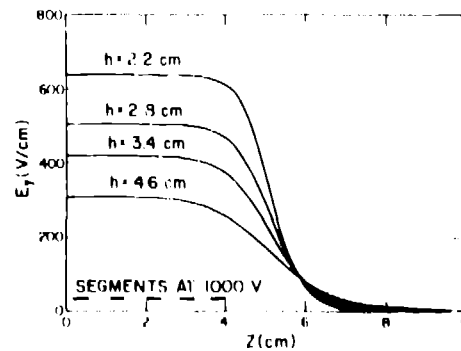


Fig. 4. Electric field on-axis at the wavefront of Fig. 1, calculated for four values of deflector spacing h . The step-function pulse ends at $Z = 4$ cm.

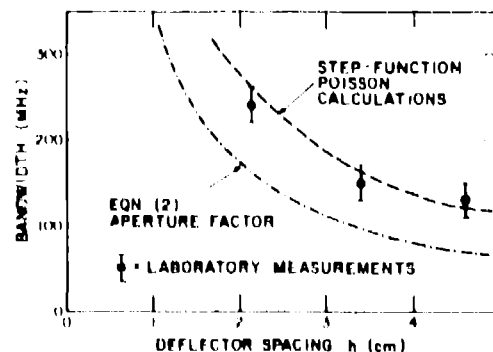


Fig. 5. Slow-wave bandwidth for deflectors. POISSON results from Fig. 4 are compared to the analytic expression and laboratory measurements.

that gave better pulse-propagation characteristics than Helix II. A meander line with copper segments on a high-dielectric substrate was discarded because the pulse direction on adjacent segments caused magnetic and electric coupling effects to add in the direction of beam propagation. A tapped coaxial line was considered, but capacitive coupling between adjacent plates resulted in large waveform distortion. These investigations resulted in a structure that uses a combination of the helix design and coaxial cable.

Figure 6 is a photograph of what we call the coax-plate design, which uses flat plates on the structure's beam side soldered to and supported by short lengths of coaxial cable that connect adjacent plates across the back of the ground plane. The cables' lengths are adjusted to match pulse propagation to beam velocity. The plate width and spacing can thus be chosen to give the best compromise between efficiency and coupling. Because the coaxial cable provides most of the path length, deleterious effects from mismatch at the corners, as well as coupling between turns on the structure's back, are avoided. The plates' shape and spacing from the ground plane are adjusted empirically, providing 50- Ω impedance with minimum perturbation at the coaxial cable transition. Individual plate replacement is accomplished easily without disturbing the rest of the structure.

The plates' thickness influences plate-to-plate coupling; therefore, we used 0.4-mm-thick spring steel for desirable stiffness, copper plated for conductivity. We can thus maximize efficiency by making the plates 7.9 mm wide on a 10.2-mm center-to-center spacing for a 78% aspect ratio and a 94% calculated dc efficiency (Fig. 3). The chopper's bandwidth, with an assumed spacing h of 2.8 cm between deflecting structures, is ~ 200 MHz (Fig. 5). This bandwidth improves the field characteristics on-axis by attenuating the 500-MHz signals generated by turn-to-turn coupling. The field measurement of a step-function pulse applied to a 30-cm-long segment of the coax-plate structure is compared to the input and output pulses on the transmission line in Fig. 7.

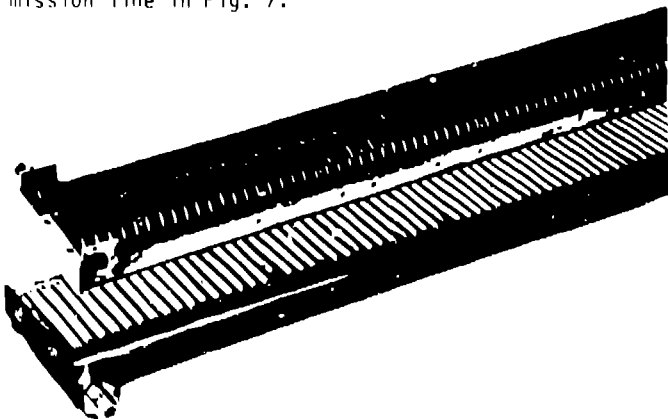


Fig. 6. Photograph of coax-plate structure.

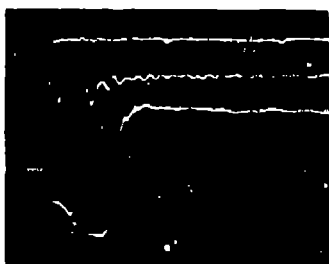


Fig. 7. Upper trace is input pulse, middle is output, and lower is field measurement of coax-plate deflector. Time scale is 5 ns/division.

Power Amplifiers

Two power amplifiers (positive output and negative output) with the following characteristics are required for driving the deflection structures.

Rise and fall times	<5 ns
Voltage output into 50 Ω	>600 V
Pulse width	<15 ns to >1 ms
Duty factor	10% maximum
Time jitter	<1 ns

An amplifier configuration using planar triodes and VMOS FETs in a parallel cascode arrangement was chosen to meet these requirements. The cascode configuration takes advantage of the low output capacitance and high voltage-swing capability of the triode and wide bandwidth transconductance of the rf VMOS FET.

Figure 8 shows a simplified diagram of the power-amplifier and deflector system. The amplifiers are operated on isolated decks in order for the deflector base line to be at ground potential. To produce the positive drive, the negative tube output is inverted by a transmission-line transformer. To prevent excessive droop for a 1-ms pulse, the amplifier is isolated from ground by a low-capacitance isolation transformer and a fiber-optic signal link. Figure 9 shows the pulse response of a power amplifier.

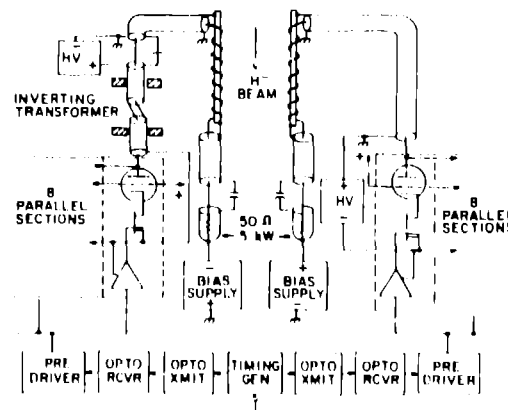


Fig. 8. Power amplifier simplified block diagram.



Fig. 9. Response of the power amplifier for 600-V pulse. Time scale is 10 ns/division.

References

1. R. F. Bentley, J. S. Lunsford, and G. P. Lawrence, "Pulsed Beam Chopper for LAMPF," IEE Trans. Nucl. Sci. 22, No. 3, p. 1526 (1975).
2. J. S. Lunsford, G. P. Lawrence, and R. F. Bentley, "Versatile H⁺ Beam Chopper System at LAMPF," IEE Trans. Nucl. Sci. 26, No. 3, p. 3433 (1979).
3. L. A. Roberts, R. Miller, D. J. Bates, "LAMPF Proton Beam Chopper Study," Watkins-Johnson Company report, Project No. 6350, May 1973.
4. R. A. Hardekopf and J. S. Lunsford, "Measurements and Calculations of HELIX II Beam Chopper Parameters," Los Alamos National Laboratory, Accelerator Technology Division, PSR Technical Note No. 107 (June, 1982).